A primal-dual algorithm for computing finsler distances and applications

Hamza Ennaji, Yvain Quéau, Abderrahim Elmoataz

A PRIMAL-DUAL ALGORITHM FOR COMPUTING FINSLER DISTANCES AND APPLICATIONS

HAMZA ENNAJI, YVAIN QUÉAU AND ABDERRAHIM ELMOATAZ†

ABSTRACT. This note discusses the computation of the distance function with respect to Finsler metrics. To this end, we show how the Finsler variants of the Eikonal equation can be solved by a primal-dual algorithm exploiting the variational structure. We also discuss the acceleration of the algorithm by preconditioning techniques, and illustrate the flexibility of the proposed method through a series of numerical examples.

1. INTRODUCTION

Computing the distance function to a target set plays a central role in geometry and arises in many applications such as path planning, meshing, image processing, shape detection of tumors from medical images, tractography or neural fiber tracking in neuroscience (see e.g., [40, 41, 49, 25, 16, 32, 31] and the references therein).

A first example is the computation of geodesics. Given a domain $\Omega \subset \mathbb{R}^N$, and $\mathbf{x}, \mathbf{y} \in \Omega$, the geodesic distance between $\mathbf{x}$ and $\mathbf{y}$ is defined through

$$d(\mathbf{x}, \mathbf{y}) = \inf_{\gamma \in \Gamma(\mathbf{x},\mathbf{y})} L(\gamma), \tag{1.1}$$

where $\Gamma(\mathbf{x}, \mathbf{y}) = \{\gamma \in W^{1,1}([0,1], \overline{\Omega}), \gamma(0) = \mathbf{x}, \gamma(1) = \mathbf{y}\}$, $L(\gamma)$ is the so called length (or action) functional of $\gamma \in \Gamma(x, y)$ given by

$$L(\gamma) = \int_0^1 |\dot{\gamma}(t)| \mathrm{d}t.$$

It is well known that (1.1) admits a solution (provided $\Gamma(\mathbf{x}, \mathbf{y})$ is nonempty) γ which is of minimal length, i.e., $d(\mathbf{x}, \mathbf{y}) = L(\gamma)$. Moreover, given a closed $C \subset \Omega$, $d(., C) = \inf_{\mathbf{y} \in C} |\cdot - \mathbf{y}|$ is the unique viscosity solution of the Eikonal equation (see e.g., [33])

$$\|\nabla u\| = 1 \text{ in } \Omega \setminus C, \text{ and } u = 0 \text{ on } C. \tag{1.2}$$

Then, the geodesic γ between some point $\mathbf{x}_0 \in \Omega$ and any point of C is characterized by the following ordinary differential equation (ODE)

$$\dot{\gamma}(t) = -\frac{\nabla d(\gamma(t), C)}{\|\nabla d(\gamma(t), C)\|}, \text{ with } \gamma(0) = \mathbf{x}_0.$$

Date: March 25, 2022.

†Normandie Univ, UNICAEN, ENSICAEN, CNRS, GREYC, France. Emails: hamza.ennaji@unicaen.fr, yvain.queau@ensicaen.fr, abderrahim.elmoataz@unicaen.fr.

Another classic example, arising from control theory, is the minimum time problem, where one seeks to steer some dynamics

$$\dot{\mathbf{y}}(t) = f(\mathbf{y}(s), \alpha(t)), \text{ and } \mathbf{y}(t_0) = \mathbf{y}_0 \in \mathbb{R}^N, \tag{1.3}$$

in the shortest possible time to a given target $C \subset \mathbb{R}^N$, where $t_0 \in \mathbb{R}$, α is an admissible control and f is a continuous function satisfying the classical Caratheodory's theorem assumptions (see e.g., [6]) ensuring the existence and uniqueness of a global solution to (1.3). Then, the first arrival time to C is defined through $T_{\mathbf{x}}(\alpha) = \inf_t \{t > 0 : \ \mathbf{y}(t, \alpha) \in C\}$ and the value function of the minimum time problem is given by

$$T(\mathbf{x}) = \inf_{\alpha} T_{\mathbf{x}}(\alpha).$$

Then, thanks to the dynamic programming principle (see e.g., [6]), T satisfies the following boundary value problem:

$$\mathrm{H}(\mathbf{x}, \nabla u) = 0 \ \text{ in } \mathcal{R} \setminus C, \ \text{ and } \ u = 0 \ \text{ on } \partial C,$$

where $\mathcal{R} = \{x \in \mathbb{R}^N : \ T(x) < \infty\}$ and $\mathrm{H}(\mathbf{x}, \mathbf{p}) = \sup_a \{-\mathbf{p} \cdot f(\mathbf{x}, a) - 1\}$.

In both examples, the starting point is to compute the distance function, i.e., , to solve a Hamilton-Jacobi (HJ) equation. HJ equations, particularly of the Eikonal type, are also at the core of many geodesic-related problems in imaging, and have been widely considered in skeleton and Voronoi computation [27, 47], active contours and segmentation [30, 39, 12, 11, 10, 9] and in many other applications (see e.g., [40, 41] and the references therein). One of the key challenges arising in such applications is to design HJ solvers which are both efficient and able to handle general (non-Euclidean) metrics.

The most famous methods for solving Euclidean HJ equations remain the Fast Marching Method (FMM) [45, 48], the Fast Sweeping Method (FSM) [35, 50] and semi-Lagrangian schemes [21]. Heat methods based on Hopf-Cole transform were proposed in [14, 15], and p-Laplace approximations were considered in [23]. This approach can be extended to general Finsler metrics thanks to [19]. For more general metrics, generalization of the FMM has been proposed in [38, 36, 37] using Voronoi's first reduction. More closely related to our work are ADMM methods, which have proven very effective for computing distance function in the Euclidean case [4, 23] but have not been extended yet to general Finsler metrics.

Contributions and organization of the paper. In this note, we introduce an efficient primal-dual framework for the computation of Finsler distances, based on a variational reformulation of Finsler variants of the Eikonal equation (1.2). We also discuss several strategies to accelerate the algorithm, and revisit different type of metrics that are present in the literature: Euclidean, Riemannian, Randers metrics and ones appearing in transportation theory such as crystalline metrics. For each metric, we give details concerning projections onto sublevels, which represents the main step in the proposed algorithm. The paper is organized as follows. In Section 2 we recall some facts on HJ equations and we present the variational formulation that will be used to compute the distance function. In Section 3 we present a discrete variant of our variational formulation and introduce a PD algorithm for solving it. In Section 4 we give several examples of distance computations and geodesic extractions, for a variety of metrics. Finally, we draw our conclusions and discuss possible extensions in Section 5.

Notations. Throughout this note, Ω is a bounded regular domain of $\mathbb{R}^N$ ($N = 2$ in Section 4). We use bold notation for vectors, i.e., $\mathbf{p} \in \mathbb{R}^N$. We write $\mathbf{x} = (x, y)$ for $\mathbf{x} \in \Omega \subset \mathbb{R}^2$. We denote by $\|\cdot\|$ the Euclidean norm on $\mathbb{R}^N$ and by $\mathcal{S}_N^{++}$ the set of symmetric positive definite matrices. Given $M \in \mathcal{S}_N^{++}$, we denote $\langle \mathbf{p}, \mathbf{q} \rangle_M = \langle \mathbf{p}, M\mathbf{q} \rangle$ and $\|\mathbf{p}\|_M = \langle \mathbf{p}, \mathbf{p} \rangle_M^{1/2}$.

2. HJ EQUATION AND THE DISTANCE FUNCTION

2.1. **Reminders on HJ equations.** Given a bounded regular domain $\Omega \subset \mathbb{R}^N$, we consider a continuous Hamiltonian $\mathrm{H} : \overline{\Omega} \times \mathbb{R}^N \to \mathbb{R}$ such that for every $\mathbf{x} \in \overline{\Omega}$

$$\{\mathbf{q} \in \mathbb{R}^n : \ \mathrm{H}(\mathbf{x}, \mathbf{q}) \leq 0\} \triangleq Z(\mathbf{x}) \ \text{ is convex, compact and contains the origin,} \tag{2.4}$$

and consider the following HJ equation:

$$\mathrm{H}(\mathbf{x}, \nabla u) = 0, \ \ x \in \Omega. \tag{2.5}$$

We recall the following definition:

Definition 2.1. A continuous function $u \colon \Omega \to \mathbb{R}$ is said to be

- a viscosity subsolution of (2.5) in Ω if $H(\mathbf{x}, \mathbf{q}) \leq 0$ for every $\mathbf{x} \in \Omega$ and every $\mathbf{q} \in D^+u(\mathbf{x})$,
- a viscosity supersolution of (2.5) in Ω if $H(\mathbf{x}, \mathbf{q}) \geq 0$ for every $\mathbf{x} \in \Omega$ and every $\mathbf{q} \in D^-u(\mathbf{x})$,
- a viscosity solution of (2.5) in Ω if it is both a subsolution and supersolution.

Recall that here, $D^+u(\mathbf{x})$ and $D^-u(\mathbf{x})$ stand, respectively, for the superdifferential and subdifferential of u at $\mathbf{x}$ and are given by

$$D^+u(\mathbf{x}) = \left\{ \mathbf{q} \in \mathbb{R}^N : \ \limsup_{|v| \to 0} \frac{u(\mathbf{x}+\mathbf{v}) - u(\mathbf{x}) - \langle \mathbf{q}, \mathbf{v} \rangle}{|\mathbf{v}|} \leq 0 \right\},$$

$$D^-u(\mathbf{x}) = \left\{ \mathbf{q} \in \mathbb{R}^N : \ \liminf_{|v| \to 0} \frac{u(\mathbf{x}+\mathbf{v}) - u(\mathbf{x}) - \langle \mathbf{q}, \mathbf{v} \rangle}{|\mathbf{v}|} \geq 0 \right\}.$$

We refer the reader to [13, 33] for more details on the theory of viscosity solutions for HJ equations.

The support function of the 0-sublevels set $Z(\mathbf{x})$ is defined through

$$\sigma(\mathbf{x}, \mathbf{q}) = \sup_{\mathbf{q} \in Z(\mathbf{x})} \langle \mathbf{q}, \mathbf{q} \rangle, \tag{2.6}$$

which is a Minkowski norm on $\overline{\Omega} \times \mathbb{R}^N$ and thus defines a Finsler metric on $\mathbb{R}^N$.

Assumption (2.4) ensures that σ is a possibly degenerate Finsler metric, i.e., we may have $\sigma(\mathbf{x}, \mathbf{q}) = 0$ for $\mathbf{q} \neq 0$, and its dual σ^*, defined by

$$\sigma^*(\mathbf{x}, \mathbf{q}) := \sup_{\mathbf{q}} \{ \langle \mathbf{q}, \mathbf{q} \rangle : \ \sigma(\mathbf{x}, \mathbf{q}) \leq 1 \}, \tag{2.7}$$

may take the value $+\infty$ (we call it a weak Finsler metric). Consequently, σ may fail to be equivalent to the Euclidean distance. In other words, there exists $K > 0$ such that

$$0 \leq \sigma(\mathbf{x}, \mathbf{q}) \leq K|\mathbf{q}| \text{ for } \mathbf{x} \in \overline{\Omega}, \ \ \mathbf{q} \in \mathbb{R}^N.$$

We then define the intrinsic distance by

$$d_\sigma(\mathbf{x},\mathbf{y}) := \inf_{\zeta\in\Gamma(\mathbf{x},\mathbf{y})} \int_0^1 \sigma(\zeta(t),\dot\zeta(t))\,\mathrm{d}t, \tag{2.8}$$

which is a quasi-distance, i.e., satisfying $d_\sigma(\mathbf{x},\mathbf{x}) = 0$ and the triangular inequality, but not necessarily symmetric. In addition, due to Assumption (2.4), it may happen that $d_\sigma(\mathbf{x},\mathbf{y}) = 0$ for $\mathbf{x} \neq \mathbf{y}$. The following proposition summarizes some basic characterizations of subsolutions in terms of d_σ.

Proposition 2.2. *([18, 22])*

1) *Compatibility condition: v is a subsolution of (2.5) in Ω if and only if $v(\boldsymbol{x}) - v(\boldsymbol{y}) \leq d_\sigma(\boldsymbol{y},\boldsymbol{x})$ for any $\boldsymbol{x},\boldsymbol{y} \in \Omega$.*
2) *We have*
$$u(\boldsymbol{x}) - u(\boldsymbol{y}) \leq d_\sigma(\boldsymbol{y},\boldsymbol{x}) \Longleftrightarrow \sigma^*(\boldsymbol{x},\nabla u) \leq 1 \ \text{ a.e. in } \Omega.$$

After these reminders on the metric character of HJ equation, we are now in position to introduce the variational formulation that will allow recovering the distance function with respect to general Finsler metric.

2.2. **Characterization of the distance function.** Given a closed subset $C \subset \overline{\Omega}$ (typically $C = \partial\Omega$ or $C = \{\mathbf{x}_0\}$ for some $\mathbf{x}_0 \in \overline{\Omega}$), we consider the following HJ equation:

$$\begin{cases} \mathrm{H}(\mathbf{x},\nabla u) = 0 & \text{in } \Omega, \\ u = g & \text{on } C, \end{cases} \tag{2.9}$$

where $g : C \to \mathbb{R}$ is a continuous function satisfying the compatibility condition

$$g(\mathbf{x}) - g(\mathbf{y}) \leq d_\sigma(\mathbf{y},\mathbf{x}) \quad \text{for any } \mathbf{x},\mathbf{y} \in C.$$

We know then that the maximal viscosity subsolution is given by

$$\mathrm{D}(\mathbf{x}) = \min_{\mathbf{y}\in C} \left\{ d_\sigma(\mathbf{y},\mathbf{x}) + g(\mathbf{y}) \right\}, \tag{2.10}$$

which, thanks to Proposition 2.2, can be recovered via the following maximization problem:

$$\max \left\{ \int_\Omega u\,\mathrm{d}\mathbf{x} \ : \ u(\mathbf{x}) - u(\mathbf{y}) \leq d_\sigma(\mathbf{y},\mathbf{x}),\ \forall \mathbf{x},\mathbf{y} \in \Omega \text{ and } u = g \text{ on } C \right\},$$

where $d_\sigma(.,.)$ is the intrinsic distance associated to the Hamiltonian, as defined in (2.8). Equivalently (cf. [18, Theorem 2.6]), we have that (2.10) is the unique solution of the following maximization problem:

$$\max_{v\in W^{1,\infty}(\Omega)} \left\{ \int_\Omega v\,\mathrm{d}x,\ \sigma^*(\mathbf{x},\nabla v(\mathbf{x})) \leq 1 \text{ and } v = g \text{ on } C \right\}. \tag{2.11}$$

The advantage of this variational formulation is that it turns the PDE (2.9) into an optimization problem for which efficient highly efficient solvers exist. Taking $g \equiv 0$, this provides a practical way to recover the distance function with respect to several Finsler metrics.

3. Numerical approximation

In this section we present the main ingredients to derive a discrete version of the variational problem (2.11) and we write it in a suitable form to use a primal dual algorithm (PD for short) to approximate the distance function. We also discuss some preconditioning techniques that could help improving the results.

3.1. **Discretization and formulation.** Following [7], we discretize the domain Ω using a regular grid $m \times n$: $\{(ih, jh) : 1 \leq i \leq m, 1 \leq j \leq n\}$ for a fixed $h > 0$. We denote by $C_d = \{(i,j) : (ih, jh) \in C\}$ the indices whose spatial positions belong to C and by $u_{i,j}$ the values of u at (ih, jh). The space $X = \mathbb{R}^{m\times n}$ is equipped with a scalar product and an associated norm as follows:

$$\langle u, v\rangle = h^2 \sum_{i=1}^{m}\sum_{j=1}^{n} u_{i,j}v_{i,j} \quad \text{and} \quad \|u\| = \sqrt{\langle u, u\rangle}.$$

For $1 \leq i \leq m$ and $1 \leq j \leq n$, we define the components of the discrete gradient operator via finite differences:

$$(\nabla_h u)^1_{i,j} = \begin{cases} \dfrac{u_{i+1,j} - u_{i,j}}{h} & \text{if } i < m, \\ 0 & \text{if } i = m, \end{cases} \quad \text{and} \quad (\nabla_h u)^2_{i,j} = \begin{cases} \dfrac{u_{i,j+1} - u_{i,j}}{h} & \text{if } j < n, \\ 0 & \text{if } j = n. \end{cases}$$

Then the discrete gradient $\nabla_h : X \longrightarrow Y = \mathbb{R}^{m\times n\times 2}$ is given by $(\nabla_h u)_{i,j} = \left((\nabla_h u)^1_{i,j}, (\nabla_h u)^2_{i,j}\right)$ and its adjoint, the discrete divergence operator $\mathrm{div}_h : Y \to X$, is given by

$$(\mathrm{div}_h \phi)_{i,j} = \begin{cases} \dfrac{\phi^1_{1,j}}{h} & \text{if } i = 1, \\ \dfrac{\phi^1_{i,j} - \phi^1_{i-1,j}}{h} & \text{if } 1 < i < m, \\ \dfrac{-\phi^1_{m-1,j}}{h} & \text{if } i = m, \end{cases} + \begin{cases} \dfrac{\phi^2_{i,1}}{h} & \text{if } j = 1, \\ \dfrac{\phi^2_{i,j} - \phi^2_{i,j-1}}{h} & \text{if } 1 < j < n, \\ \dfrac{-\phi^2_{i,n-1}}{h} & \text{if } j = n. \end{cases}$$

Proposition 3.3. *([7, 8]) Under the aforementioned definitions and notations, one has that*

- *The adjoint operator of ∇_h is $\nabla_h^* = -\mathrm{div}_h$.*
- *Its norm satisfies: $\|\nabla_h\|^2 = \|\mathrm{div}_h\|^2 \leq 8/h^2$.*

This suggests considering the following discrete version of the variational problem (2.11):

$$\min_{\substack{u\in X \\ u_{i,j}=g_{i,j}\ \forall (i,j)\in C_d}} \left\{ -h^2 \sum_{i=1}^{m}\sum_{j=1}^{n} u_{i,j} + \mathbb{I}_{B_{\sigma^*}}(\nabla_h u)\right\} \tag{3.12}$$

where $\mathbb{I}_{B_{\sigma^*}}$ is the indicator function of $B_{\sigma^*} := \left\{v \in Y : \sigma^*(ih, jh, v_{i,j}) \leq 1,\ \forall (i,j)\right\}$ the unit ball w.r.t. σ^*, that is

$$\mathbb{I}_{B_{\sigma^*}}(v) = \begin{cases} 0 & \text{if } v \in B_{\sigma^*} \\ +\infty & \text{otherwise.} \end{cases}$$

In other words, the discrete optimization problem (3.12) can be written as

$$\min_{u\in X} \mathcal{F}_h(u) + \mathcal{G}_h(\nabla_h u), \tag{3.13}$$

where

$$\mathcal{F}_h(u) = \begin{cases} -h^2 \sum_{i=1}^{m}\sum_{j=1}^{n} u_{i,j} \text{ if } u = g \text{ on } C_d, \\ +\infty \text{ otherwise,} \end{cases} \qquad \text{and} \qquad \mathcal{G}_h(v) = \mathbb{I}_{B_{\sigma^*}}.$$

Besides, (3.12) can be rewritten in a dual form (see [20, 18]) involving the total variation of some vector measure fields ϕ with respect to the metric σ. More precisely, the dual problem is a minimal flow type problem given by

$$\min_{\substack{\phi\in Y \\ (-\mathrm{div}_h\phi)_{i,j}=1 \text{ for } (i,j)\notin C_d}} h^2 \Bigg\{ \sum_{i=1}^{m}\sum_{j=1}^{n} \sigma(ih, jh, \phi_{i,j}) + \sum_{(i,j)\in C_d} g_{i,j}\left((\mathrm{div}_h\phi)_{i,j} + 1\right) \Bigg\}. \tag{3.14}$$

The duality between (3.12) and (3.14) gives particularly a characterization of the distance function. More precisely, the pair $(u, \phi) \in X \times Y$ solves the primal and dual problems if and only if (see e.g., [17])

$$\mathrm{div}_h(\phi) \in \partial\mathcal{F}_h(u) \text{ and } \phi \in \partial\mathcal{G}_h(\nabla_h u),$$

that is,

$$\begin{cases} -(\mathrm{div}(\phi))_{i,j} = 1 & \text{for all } (i,j) \notin C_d, \\ \phi_{i,j}\cdot\nabla_h u_{i,j} = \sigma(ih, jh, \phi_{i,j}) & \text{for all } (i,j), \\ u_{i,j} = g_{i,j} & \text{for all } (i,j) \in C_d. \end{cases} \tag{3.15}$$

Lastly, a primal-dual formulation of the primal problem (3.12) reads (see e.g., [44] for details)

$$\inf_{u\in X}\sup_{\phi\in Y} \mathcal{F}_h(u) + \langle\phi, \nabla_h u\rangle - \mathcal{G}_h^*(\phi),$$

and the latter form can be solved using the following general (PD) algorithm:

Algorithm 1 PD algorithm [8]

1st step. Initialization: choose $\eta, \tau > 0$, $\theta \in [0,1]$, u^0 and take $\phi^0 = \nabla_h u^0$, $\bar{u}^0 = u^0$.
2nd step. For $k \le \mathrm{Iter}_{max}$ do

$$\begin{aligned} \phi^{k+1} &= \mathbf{Prox}_{\eta\mathcal{G}_h^*}(\phi^k + \eta\nabla_h(\bar{u}^k)); \\ u^{k+1} &= \mathbf{Prox}_{\tau\mathcal{F}_h}(u^k - \tau\nabla_h^*(\phi^{k+1})); \\ \bar{u}^{k+1} &= u^{k+1} + \theta(u^{k+1} - u^k). \end{aligned}$$

It was shown in [8] that when $\theta = 1$ and $\eta\tau\|\nabla_h\|^2 < 1$, the sequence $\{(u^k, \phi^k)\}$ generated by Algorithm 1 converges to an optimal solution of (3.13). This algorithm has been widely used especially in image processing and optimal transport fields.

3.2. **Computation of the proximal operators.** As one sees, in order to apply Algorithm 1 one needs to compute the proximal operators of the functions $\mathcal{F}_h$ and $\mathcal{G}_h^*$. Recall that for a convex, lower-semicontinuous and proper function K, the proximal operator (also called resolvent operator) reads

$$\mathbf{Prox}_{\tau K}(u) = \underset{v}{\operatorname{argmin}} \frac{1}{2}\|u - v\|^2 + \tau K(v), \tau > 0.$$

For $K = \mathcal{F}_h$ and $K = \mathcal{G}_h^*$, $\mathbf{Prox}_K$ can be computed explicitly. In particular, we have

$$\mathbf{Prox}_{\tau\mathcal{F}_h}(u) = \underset{v\in X}{\operatorname{argmin}} \frac{1}{2}\|v - u\|^2 + \tau\mathcal{F}_h(v) = \underset{v=g \text{ on } C_d}{\operatorname{argmin}} \frac{1}{2}\|v - u\|^2 - \tau h^2 \sum_{i=1}^{m}\sum_{j=1}^{n} v_{i,j}.$$

The optimal solution is reached when the derivative of the objective function vanishes. A straightforward computation gives:

$$(\mathbf{Prox}_{\tau\mathcal{F}_h}(u))_{i,j} = \begin{cases} u_{i,j} + \tau \text{ for } (i,j) \notin C_d, \\ g_{ij} \text{ for } (i,j) \in C_d. \end{cases}$$

In order to compute $\mathbf{Prox}_{\eta\mathcal{G}_h^*}$ we first observe that $\mathbf{Prox}_{\eta^{-1}\mathcal{G}_h}$ is nothing but the projection onto B_{σ^*} since

$$\begin{aligned} \mathbf{Prox}_{\eta^{-1}\mathcal{G}_h}(\psi) &= \underset{\mathbf{q}\in Y}{\arg\min} \frac{1}{2}\|\mathbf{q} - \psi\|^2 + \frac{1}{\eta}\mathcal{G}_h(\mathbf{q}) \\ &= \underset{q_{i,j}\in B_{\sigma^*}}{\arg\min} \frac{1}{2}\|\mathbf{q} - \psi\|^2 \\ &= \mathbf{Proj}_{B_{\sigma^*}}(\psi). \end{aligned}$$

Then, using Moreau's identity

$$\phi = \mathbf{Prox}_{\eta\mathcal{G}_h^*}(\phi) + \eta\mathbf{Prox}_{\eta^{-1}\mathcal{G}_h}(\phi/\eta), \ \forall \phi \in Y,$$

we get

$$\Big(\mathbf{Prox}_{\eta\mathcal{G}_h^*}(\psi)\Big)_{i,j} = \psi_{i,j} - \eta\mathbf{Proj}_{B_{\sigma^*}}(\psi_{i,j}/\eta), \forall i = 1, ..., m, \ j = 1, ..., n.$$

Therefore, to compute $\mathbf{Prox}_{\eta\mathcal{G}_h^*}$, it is sufficient to be able to project onto B_{σ^*}, and thus, Algorithm 1 provides a simple way to recover the distance function with respect to general Finsler metrics. This has been made possible via gauge functionals (the support function σ and its dual σ^*, see (2.6)-(2.7)) which makes the correspondence between geometrical objects (here unit balls B_{σ^*}) and analytical objects (Hamiltonians). The details of Algorithm 1 to approximate the distance function read:

Algorithm 2 Primal-dual method for the numerical approximation of the distance function

Initialization: Let $k = 0$, choose $\eta, \tau > 0$ such that $\eta\tau < \frac{8}{h^2}$. Take $u^0 = \bar{u}^0 = u_0$ and $\phi^0 = \nabla_h u^0$.

Primal step:

$$\psi^{k+1} = \phi^k + \eta \nabla_h \bar{u}^k.$$
$$\phi_{i,j}^{k+1} = \psi_{i,j}^{k+1} - \eta \mathbf{Proj}_{B_{\sigma^*}}(\psi_{i,j}^{k+1}/\eta),\ 1 \le i \le m, 1 \le j \le n.$$

Dual step:

$$v^{k+1} = u^k + \tau \mathrm{div}_h(\phi^{k+1}).$$
$$u_{i,j}^{k+1} = v_{i,j}^{k+1} + \tau,\ 1 \le i \le m, 1 \le j \le n.$$

Extragradient:

$$\bar{u}^{k+1} = 2u^{k+1} - u^k.$$

3.3. **Acceleration of the algorithm.** First, let us say that PD iterations can be improved using preconditioning and variable metrics techniques. In fact, following [42], we can consider a preconditioned version of Algorithm 2 as follows. Given $T, Q \in \mathcal{S}_{++}^N$, u_0 and ϕ^0, P-DP iterations read

$$\text{(P-PD)}: \begin{cases} \phi^{k+1} = \mathbf{Prox}_{G_h^*}^T\left(\phi^k + T\nabla_h(2u^{k+1} - u^k)\right), \\ u^{k+1} = \mathbf{Prox}_{F_h}^Q\left(u^k - Q\nabla_h^*(\phi^{k+1})\right), \end{cases} \tag{3.16}$$

where $\mathbf{Prox}_K^M(u) = \arg\min_v \frac{1}{2}\|u - v\|_M^2 + K(v)$ and $M \in \mathcal{S}_{++}^N$ is the scaled proximal operator of K relative to the metric M. To ensure the convergence of (P-PD) iterations, the preconditioners Q and T must satisfy $\|T^{\frac{1}{2}}\nabla_h Q^{\frac{1}{2}}\|^2 < 1$, which reduces to $\eta\tau\|\nabla_h\|^2 < 1$ when $T = \eta I_N$ and $Q = \tau I_N$. Since computing $\mathbf{Prox}_K^M$ is difficult in general, the choice of the preconditioner is crucial. For instance, the authors in [42] proposed a family of diagonal preconditioners as follows. For any $r \in [0, 2]$, take $T = \mathrm{diag}((\eta_i)_i)$ and $Q = \mathrm{diag}((\tau_j)_j)$ where

$$\eta_i = \frac{1}{\sum_{j=n}^N |(\nabla_h)_{i,j}|^{2-r}}, \tau_j = \frac{1}{\sum_{i=m}^N |(\nabla_h)_{i,j}|^r}.$$

To observe the difference of PD and P-PD, let us consider the Eikonal equation $|\nabla u| = k(\mathbf{x})$ in $[0, 1]^2$ with homogeneous Dirichlet boundary condition with a mesh size $h = 0.01$, and take the relative error

$$E_k := \|u_k - u_{k-1}\| / \|u_k\| < \epsilon = 10^{-6}$$

as a stopping criterion. In the case where $k \equiv 1$ (Figure 1-A), we observed that it took 5900 iterations (in 11.4 seconds[1]) for PD to stop, whereas P-PD stopped after 5500 iterations (in 10.95

[1]The numerical examples were executed on a M1 CPU running MacOs Monterey system. Demonstration code is available at https://github.com/enhamza/pd_eikonal.

seconds). In the case where

$$k(\mathbf{x}) = 2\pi\sqrt{\cos(2\pi x)^2\sin(2\pi y)^2 + \cos(2\pi y)^2\sin(2\pi x)^2}$$

(Figure 1-B), PD stopped after 2900 iterations (in 5.6 seconds), while the P-PD stopped after 2800 (in 5.5 seconds).

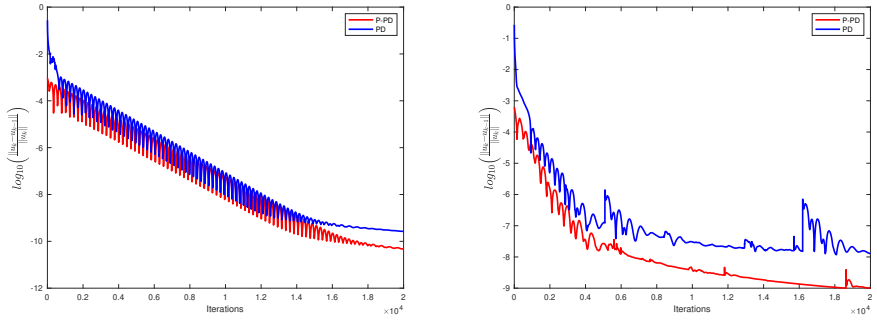

(A) Euclidean case (B) Riemannian case

FIGURE 1. Comparison between the convergence of primal-dual and preconditioned primal-dual iterations, for two types of distances.

Figure 1 shows that the relative error E_k is smaller from the beginning of the iterations when considering a preconditioner. We can also observe that the speed on convergence is affected by the smoothness of the metric. We believe that use of non-diagonal preconditioning and subproblem procedures (like solving the u-subproblem in (3.16) using proximal-gradient descent) could lead to improved results (see e.g., [34]). We are planing to investigate this in depth in future work.

4. NUMERICAL EXPERIMENTS

In this section we give several examples by computing the distance function using different Finsler metrics $F : \overline{\Omega} \times \mathbb{R}^N \to \mathbb{R}^+$, and the following HJ equation:

$$\begin{cases} F^*(\mathbf{x}, \nabla u) = 1 \text{ in } \Omega \setminus C, \\ u = 0 \text{ on } C. \end{cases} \tag{4.17}$$

Let D_C be the distance function to C (given by (2.10)) obtained by solving (4.17). Then, the geodesic curve between a point $x \in \Omega$ and its closest point in C satisfies

$$\dot{\gamma}(t) = -\nabla F^*(\gamma(t), \nabla D_C(\gamma(t))), \ \gamma(0) = \mathbf{x}. \tag{4.18}$$

As one can sees, Equation (4.18) is a gradient descent on the distance map with respect to metric F^*. It can be solved using an Euler scheme. Using forward Euler discretization, one needs to solve

$$\gamma_{k+1} = \gamma_k - \eta\nabla F^*(\gamma_k, \nabla D_C(\gamma_k)),$$

where $\eta > 0$ is a step-size to be suitably chosen. However, for more accuracy it is solved in practice using the technique proposed in [36] or a Runge-Kutta method[2]. On the other hand, one can use the proximal-point algorithm using backward Euler discretization. Indeed, solving

$$\gamma_{k+1} = \gamma_k - \eta \nabla F^*(\gamma_{k+1}, \nabla D_C(\gamma_{k+1})),$$

amounts to minimizing

$$\frac{1}{2\eta}\|\gamma_k - \mathbf{x}\|^2 + F^*(\mathbf{x}, \nabla D_C(\mathbf{x})).$$

That is: $\gamma_{k+1} = \mathbf{Prox}_{\eta F^*(\cdot, \nabla D(\cdot))}(\gamma_k)$.

4.1. **First examples.** We provide several examples on the Euclidean space with different metrics. More precisely, we consider the following examples (cf. Figure 2):

- Euclidean metric: $F(\mathbf{x}, \mathbf{p}) = \|\mathbf{p}\|$.
- Riemannian metric: $F(\mathbf{x}, \mathbf{p}) = k(\mathbf{x})\|\mathbf{p}\|$ with $k > 0$.
- Crystalline metric: $F(\mathbf{x}, \mathbf{p}) = \max_{i=1,\cdots,m} \langle \mathbf{p}, s_i \rangle$ for given directions s_i.
- Randers metric: $F(\mathbf{x}, \mathbf{p}) = \langle A\mathbf{p}, \mathbf{p} \rangle^{1/2} + \langle b(\mathbf{x}), \mathbf{p} \rangle$, where $A \in \mathcal{S}^N_{++}$ and $b \in \mathbb{R}^N$ such that $\|b\|_{A^{-1}} < 1$.

We also illustrate via a quadratic Hamiltonian how to recover the distance function in a more general setting.

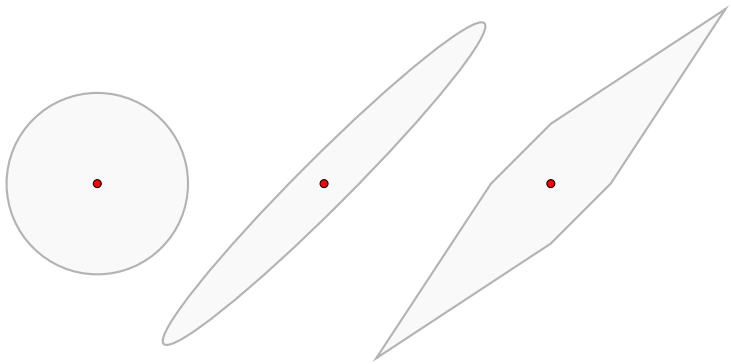

FIGURE 2. Examples of unit balls B_{F^*}. From left to right: Euclidean unit ball , unit ball for an Anisotropic Riemannian metric and the unit ball of crystalline norm.

Euclidean and Riemannian metrics. In the examples illustrated in Figure 3, the primal step in Algorithm 2 amounts to perform projections onto Euclidean balls, that is

$$\mathbf{Proj}_{B_{F^*}}(\mathbf{q}) = \begin{cases} \mathbf{q} \text{ if } \|\mathbf{q}\| \leq k, \\ k\dfrac{\mathbf{q}}{\|\mathbf{q}\|} \text{ otherwise,} \end{cases}$$

where k is the radius of the ball.

[2]In particular, we make use of a prebuilt function in the toolbox [26].

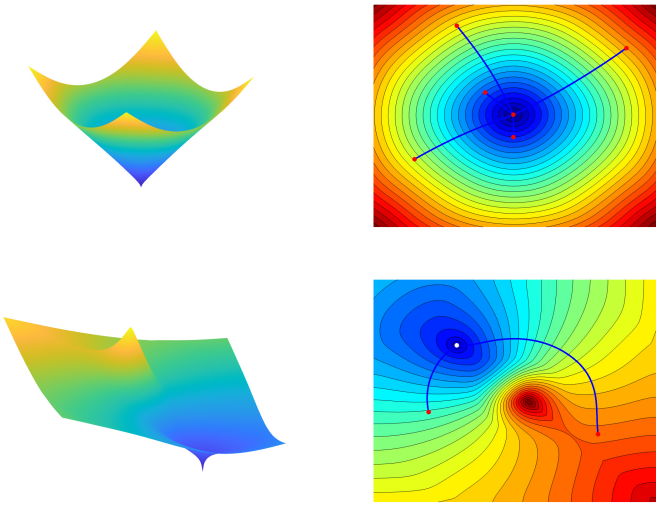

FIGURE 3. Top row: 3d-shape of the distance function computed with a single starting point with $F(\mathbf{x},\mathbf{p}) = \|\mathbf{p}\|$ (Euclidean distance), and geodesic curves between several points and the starting point displayed on the contours of the distance functions. Bottom row: 3d-shape of the distance function computed with two starting points with $F(\mathbf{x},\mathbf{p}) = k(\mathbf{x})\|\mathbf{p}\|$ and $k(\mathbf{x}) = 1 + 8e^{\frac{-x^2-y^2}{2\mu^2}}$ for $\mu > 0$ (Riemannian case), and geodesic curves. Note that in both cases, the curves are orthogonal to the contours.

Crystalline metrics. Now we consider $F(\mathbf{x},\mathbf{p}) = \max_{i=1,\cdots,5} \langle \mathbf{p}, s_i \rangle$, usually called a crystalline norm (see Figure 4). Let us denote by $v_1,\cdots,v_5$ the vertices of the unit ball of F, i.e., $B_F = \{\mathbf{p} \in \mathbb{R}^2 : F(\mathbf{p}) \leq 1\}$. Then, the primal step in Algorithm 2 consists in projecting onto the polygon $B_{F^*} = \mathrm{conv}(s_1,\cdots,s_5)$, the unit ball of F^*, where F^* is the dual norm of F (which is also a crystalline norm). The vertices of B_{F^*} are orthogonal to the edges $e_i = v_i - v_{i-1}$, that is $\langle e_i, s_i \rangle = 0$ for every i.

One way to achieve this projection is the following. If a vector $q \notin B_{F^*}$, then we compute its projection onto the successive segments $[v_i, v_{i+1}]$ and choose the right one. Otherwise we proceed as in [5] by determining onto which sector q belongs. Namely, if $q \in s_i + L_i + L_{i-1}$ with $L_i = \mathbb{R}^+ v_i$, then its projection is s_i. On the other hand, if $q \in [s_i, s_{i+1}] + L_i$, then we project it onto the segment $[s_i, s_{i+1}]$ (see Figure 5).

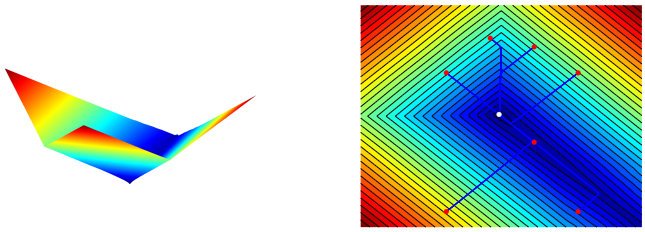

FIGURE 4. Left: 3d-shape of the distance function computed with a single starting point with a crystalline norm $F(\mathbf{x},\mathbf{p}) = \max_{i=1,\cdots,5} \langle \mathbf{p}, s_i \rangle$ with $s_1 = (1,-1), s_2 = (1,-0.8), s_3 = (-0.8,1), s_4 = (-1,1), s_5 = (-1,-1)$. Right: several geodesic curves.

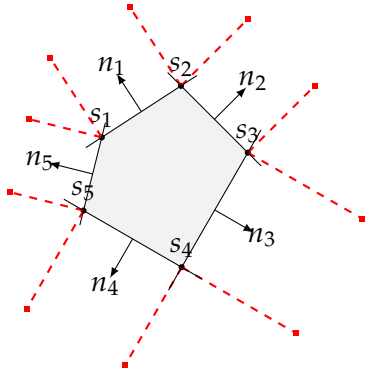

FIGURE 5. Illustration of the projection onto B_{F^*} for a crystalline norm.

Randers metrics. Another metrics are the so-called Randers metrics [43]. They are a simple example of Finsler metrics which generalize Riemannian ones and have the form $F(\mathbf{x},\mathbf{p}) = \langle A\mathbf{p},\mathbf{p}\rangle^{1/2} + \langle b(\mathbf{x}),\mathbf{p}\rangle$, where $A \in \mathcal{S}^N_{++}$ and $b \in \mathbb{R}^N$ with $\|v\|_{A^{-1}} < 1$. The first term is a Riemannian metric (anisotropic Euclidean distance) and the second term is a linear form (see e.g., [1, 46] for more details). Its dual F^* is also a Randers metric of the form (see e.g., [37, 38]) $F^*(\mathbf{x},\mathbf{p}) = \langle A_*\mathbf{p},\mathbf{p}\rangle^{1/2} + \langle b_*(\mathbf{x}),\mathbf{p}\rangle$ where

$$\delta = 1 - \langle b, A^{-1}b\rangle,\ A_* = \frac{(A^{-1}b)(A^{-1}b)^t + \delta A^{-1}}{\delta},\ b_* = -\frac{A_*^{-1}A^{-1}b}{\delta}.$$

In the example of Figure 6, we are considering a Randers metric F via its dual $\langle A\mathbf{p},\mathbf{p}\rangle^{1/2} + \langle b(\mathbf{x}),\mathbf{p}\rangle$ with

$$A = \begin{pmatrix} 0.5 & 0.6 \\ 0.6 & 1 \end{pmatrix},\ b(\mathbf{x}) = (0.3, 0.4)^t. \tag{4.19}$$

In order to project onto B_{F^*}, we may assume, up to diagonalizing A, that

$$F^*(\mathbf{x},\mathbf{p}) = \left(\sum_{i=1}^{N} \alpha_i \mathbf{p}_i^2\right)^{1/2} + \langle b(\mathbf{x}),\mathbf{p}\rangle,$$

where $\alpha_i > 0$ are the eigenvalues of A. We focus on the case where $b \equiv 0$ (otherwise the projection is obtained by translating in direction b). Then, the projection of $\mathbf{p} \in \mathbb{R}^N$ onto B_{F^*} is given by

$$\mathbf{Proj}_{B_{F^*}}(\mathbf{p}) = \begin{cases} \mathbf{p}, \text{ if } \mathbf{p} \in B_{F^*}, \\ \left(\dfrac{\alpha_1 \mathbf{p}_1}{(\alpha_1+\eta)^2}, \dots, \dfrac{\alpha_N \mathbf{p}_N}{(\alpha_N+\eta)^2}\right), \end{cases}$$

where η is the positive root of

$$f(\eta) := \sum_{i=1}^{N} \frac{\alpha_i \mathbf{p}_i^2}{(\alpha_i+\eta)^2} - 1,$$

which can be solved using a bisection method.

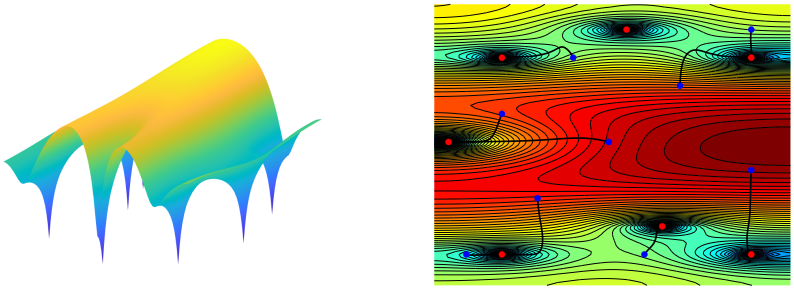

FIGURE 6. Left: 3d-shape of the distance function computed with several starting points (in white) with $F^*(\mathbf{x},\mathbf{p}) = \langle A\mathbf{p},\mathbf{p}\rangle^{1/2} + \langle b(\mathbf{x}),\mathbf{p}\rangle$ where A and b are given in (4.19). Right: geodesic curves to several end points in blue.

4.2. **General case: Projection onto level sets.** More generally, the primal step in Algorithm 2 consists in projecting onto B_{F^*}, i.e., on the $1-$sublevels of F^*. This is feasible as long as one can compute the proximal operator of F^* and find the appropriate parameter η of $\mathbf{Prox}_{\eta F^*}$. We thus recall the following

Theorem 4.4. [2, 3] *Let $Z = \{v \in \mathbb{R}^N : \mathrm{H}(v) \le c\}$ where $c \in \mathbb{R}$ and $\mathrm{H} : \mathbb{R}^N \to (-\infty,\infty]$ is a convex, proper function. If there exists $\bar{v} \in \mathbb{R}^N$ such that $\mathrm{H}(\bar{v}) < c$ then in terms of the real variable η, the equation $\mathrm{H}(\mathbf{Prox}_{\eta H}(v)) = c$ has at least one solution in $\mathbb{R}_{++}$. If $\bar{\eta}$ is such a solution, then*

$$\mathbf{Proj}_Z(v) = \mathbf{Prox}_{\bar{\eta} H(v)}.$$

To illustrate this, we suppose that the distance function is obtained by solving a HJ equation as in (2.9) with a quadratic Hamiltonian perturbed by a linear form , i.e., $\mathrm{H}(\mathbf{x},\mathbf{p}) = \dfrac{1}{2}\langle A\mathbf{p},\mathbf{p}\rangle +$

$\langle b(\mathbf{x}), \mathbf{p}\rangle - 1$, with $A \in \mathcal{S}^N_{++}$ and $b \in \mathbb{R}^N$. This kind of Hamiltonian appears typically in Freidlin-Wentzell theory of large deviations (see e.g., [28]). Moreover, we have that (see e.g., [3, Example 6.2.3])

$$\mathbf{Prox}_{\eta \mathrm{H}}(v) = (I_n + \eta A)^{-1}(v - \eta b). \tag{4.20}$$

Then, projecting onto the unit ball of F^* is given thanks to (4.20). This an advantageous formula allowing in particular to project onto ellipsoids once the optimal parameter $\bar{\eta}$ has found (usually using a bisection method). The method allows reducing additional computational costs using other algorithms as in [29].

In the example of Figure 7, we are considering $\mathrm{H}(\mathbf{x}, \mathbf{p}) = \frac{1}{2}\langle A\mathbf{p}, \mathbf{p}\rangle + \langle b(\mathbf{x}), \mathbf{p}\rangle - 1$ with

$$A = \begin{pmatrix} 1 & 0.4 \\ 0.4 & 2 \end{pmatrix}, \; b(\mathbf{x}) = (0.3, 0.4)^t. \tag{4.21}$$

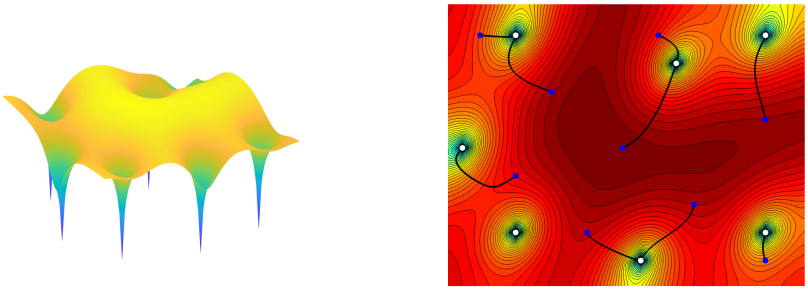

FIGURE 7. Left: 3d-shape of the distance function computed with several starting points (in white) with $\mathrm{H}(\mathbf{x}, \mathbf{p}) = \frac{1}{2}\langle A\mathbf{p}, \mathbf{p}\rangle + \langle b(\mathbf{x}), \mathbf{p}\rangle - 1$ where A and b are given in (4.21). Right: geodesic curves to several end points in blue.

4.3. **Metrics from images.** In the following examples, the metric F is constructed from an input image $I(\mathbf{x})$ in order to catch particular geodesics. In particular, we consider

$$F^*(\mathbf{x}, v) = k(\mathbf{x})^{-1}|v|,$$

were $k(\mathbf{x})$ is a potential constructed from the image[3]. For example, taking (see [40, 41]) $k(\mathbf{x}) = -I(\mathbf{x})$ or $I(\mathbf{x})$ allows recovering curves in dark and bright regions respectively. Ather possibility is to take $k(\mathbf{x}) = (\epsilon + |I(\mathbf{x}) - c|)^{-1}$ in order to get curves with constant value c, where $0 < \epsilon \ll 1$.

[3]The images are taken from [41] and can be found in https://www.numerical-tours.com/matlab/

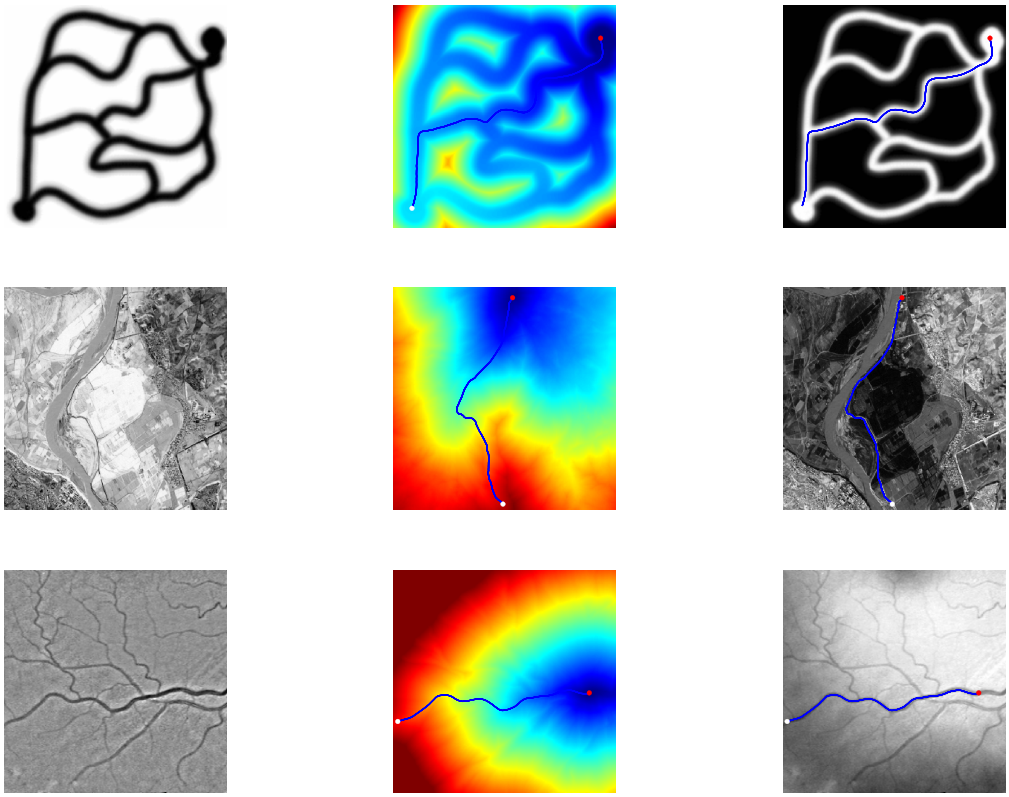

FIGURE 8. Examples of metrics (First column), the geodesic distances and curves where the starting points are in white and the endpoints in red (middle column), and the curves displayed on the image background (last column).

4.4. **Finding the shortest path to exit from a labyrinth.** In this last example we propose to find the path to exit a labyrinth by reproducing the example in [24]. The problem is usually formulated as a minimum time problem (see e.g., [6]) and thanks to the dynamic programming principle, the solution can be obtained by solving the Eikonal equation

$$\begin{cases} |\nabla u(\mathbf{x})| = k(\mathbf{x}) \text{ in } \Omega \setminus C, \\ u(\mathbf{x}) = 0 \text{ on } C, \end{cases}$$

where C represents the door and k the so-called running cost:

$$k(\mathbf{x}) = \begin{cases} \frac{1}{4} & \text{if } I(\mathbf{x}) = 1, \\ 10^{10} & \text{if } I(\mathbf{x}) = 0, \end{cases}$$

where $I(\mathbf{x})$ is a digital image representing the labyrinth (Figure 9).

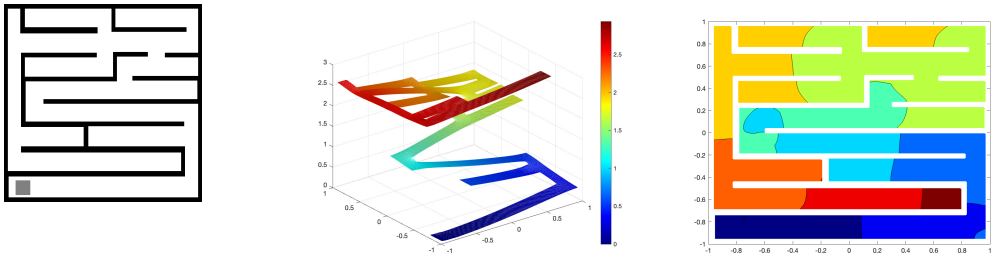

FIGURE 9. From left to right: input image $I(\mathbf{x})$ of the labyrinth (the door C is in gray), 3d-shape of the solution of the labyrinth problem function, and contours of the solutions.

5. CONCLUSIONS, COMMENTS AND EXTENSIONS

In this paper, we have proposed a primal-dual algorithm to approximate the distance function with respect to Finsler metrics with a flavor of variational formulation, which transforms the problem of estimating a distance function into solving an optimization problem. We have illustrated the flexibility of this method via different examples.

In addition to the possible improvements of the results discussed in Subsection 3.3, other applications and extensions are worth been investigated, as for instance, the extension of the proposed method to surfaces and 3D points clouds. Another application that we intend to consider in future work is the computation of skeleton or medial axis. In fact, given the distance function to the boundary of a shape S, the skeleton of S is defined as the set of singularities of the distance function $D(.)$, which in particular, solves a problem of the form

$$\max_{v\in W^{1,\infty}(\Omega)} \Big\{ \int_\Omega v\mathrm{d}x,\ F^*(\mathbf{x},\nabla v(\mathbf{x})) \leq 1 \text{ and } v = 0 \text{ on } \partial\Omega \Big\}, \tag{5.22}$$

where F is a given Finsler metric. The dual problem of (5.22) reads (see [20, 18])

$$\inf_{\Phi\in L^2(\Omega)^N} \left\{ \int_\Omega F(\mathbf{x},\Phi(\mathbf{x}))\mathrm{d}x :\ -\mathrm{div}(\Phi) = 1 \text{ in } \mathcal{D}'(\Omega) \right\}. \tag{5.23}$$

Then if the couple (u,Φ) solve (5.22)-(5.23), the complementary slackness condition (see also (3.15) for the discrete level) reads

$$\Phi(\mathbf{x}) \neq 0 \Rightarrow F^*(\mathbf{x},\nabla D(\mathbf{x})) = 1,$$

i.e., the magnitude (w.r.t F) of ∇D is binding in the support of Φ (c.f Figure 10). This observation could be used since the flow Φ is freely given by Algorithm 2 when computing the distance. We are planing to investigate theses questions in depth in future works.

Acknowledgements. This work has been funded by ANR grant Inclusive Museum Guide (ANR-20-CE38-0007).

REFERENCES

[1] D. Bao, S.-S. Chern, and Z. Shen. An introduction to Riemann-Finsler geometry, volume 200 of Graduate Texts in Mathematics. Springer-Verlag, New York, 2000. 12

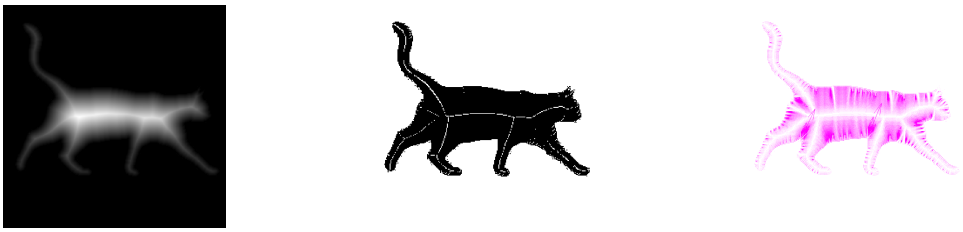

FIGURE 10. Left to right: distance to the boundary, medial axis approximated by thresholding the magnitude of the gradient, and optimal flow Φ.

[2] H. H. Bauschke and P. L. Combettes. Convex analysis and monotone operator theory in Hilbert spaces. Berlin: Springer, 2011. 13

[3] A. Beck. First-order methods in optimization, volume 25 of MOS-SIAM Series on Optimization. Society for Industrial and Applied Mathematics (SIAM), Philadelphia, PA; Mathematical Optimization Society, Philadelphia, PA, 2017. 13, 14

[4] A. Belyaev and P.-A. Fayolle. An ADMM-based scheme for distance function approximation. Numer. Algorithms, 84(3):983–996, 2020. 2

[5] J.-D. Benamou, G. Carlier, and R. Hatchi. A numerical solution to Monge's problem with a Finsler distance as cost. ESAIM, Math. Model. Numer. Anal., 52(6):2133–2148, 2018. 11

[6] P. Cannarsa and C. Sinestrari. Semiconcave functions, Hamilton-Jacobi equations, and optimal control, volume 58 of Progress in Nonlinear Differential Equations and their Applications. Birkhäuser Boston, Inc., Boston, MA, 2004. 2, 15

[7] A. Chambolle. An algorithm for total variation minimization and applications. J. Math. Imaging Vis., 20(1-2):89–97, 2004. 5

[8] A. Chambolle and T. Pock. A first-order primal-dual algorithm for convex problems with applications to imaging. J. Math. Imaging Vis., 40(1):120–145, 2011. 5, 6, 7

[9] D. Chen, J. Mirebeau, and L. D. Cohen. Finsler geodesics evolution model for region based active contours. In Proc. BMVC 2016, 2016. 2

[10] D. Chen, J.-M. Mirebeau, and L. D. Cohen. Global minimum for a Finsler elastica minimal path approach. Int. J. Comput. Vis., 122(3):458–483, 2017. 2

[11] L. Cohen and R. Kimmel. Global minimum for active contour models: a minimal path approach. In Proc. CVPR, 1996. 2

[12] L. Cohen and R. Kimmel. Regularization properties for minimal geodesics of a potential energy. In Proc. ICAOS. 1996. 2

[13] M. G. Crandall, H. Ishii, and P.-L. Lions. User's guide to viscosity solutions of second order partial differential equations. Bull. Am. Math. Soc., New Ser., 27(1):1–67, 1992. 3

[14] K. Crane, C. Weischedel, and M. Wardetzky. Geodesics in heat: A new approach to computing distance based on heat flow. ACM Trans. Graph., 32(5), oct 2013. 2

[15] K. Crane, C. Weischedel, and M. Wardetzky. The heat method for distance computation. Commun. ACM, 60(11):9099, oct 2017. 2

[16] A. Daducci, A. Marigonda, G. Orlandi, and R. Posenato. Neuronal fiber-tracking via optimal mass transportation. Commun. Pure Appl. Anal., 11(5):2157–2177, 2012. 1

[17] I. Ekeland and R. Témam. Convex analysis and variational problems, volume 28 of Classics in Applied Mathematics. Society for Industrial and Applied Mathematics (SIAM), Philadelphia, PA, english edition, 1999. Translated from the French. 6

[18] H. Ennaji, N. Igbida, and V. T. Nguyen. Augmented lagrangian methods for degenerate hamilton–jacobi equations. Calculus of Variations and Partial Differential Equations, 60(6):238, 2021. 4, 6, 16

[19] H. Ennaji, N. Igbida, and V. T. Nguyen. Quasi-convex Hamilton–Jacobi equations via limits of finsler p-Laplace problems as $p \to \infty$. July 2021. arXiv preprint: arXiv:2107.02606. 2
[20] H. Ennaji, N. Igbida, and V. T. Nguyen. Continuous Lambertian shape from shading: A primal-dual algorithm. ESAIM Math. Model. Numer. Anal., 56(2):485–504, 2022. 6, 16
[21] M. Falcone and R. Ferretti. Semi-Lagrangian approximation schemes for linear and Hamilton-Jacobi equations, volume 133. Philadelphia, PA: Society for Industrial and Applied Mathematics (SIAM), 2014. 2
[22] A. Fathi and A. Siconolfi. PDE aspects of Aubry-Mather theory for quasiconvex Hamiltonians. Calc. Var. Partial Differ. Equ., 22(2):185–228, 2005. 4
[23] P.-A. Fayolle and A. G. Belyaev. p-Laplace diffusion for distance function estimation, optimal transport approximation, and image enhancement. Comput. Aided Geom. Des., 67:1–20, 2018. 2
[24] A. Festa and M. Falcone. L^1 convergence of a SL scheme for the eikonal equation with discontinuous coefficients. In Hyperbolic problems: theory, numerics, applications, volume 8 of AIMS Ser. Appl. Math., pages 559–566. Am. Inst. Math. Sci. (AIMS), Springfield, MO, 2014. 15
[25] R. Gala, J. Chapeton, J. Jitesh, C. Bhavsar, and A. Stepanyants. Active learning of neuron morphology for accurate automated tracing of neurites. Frontiers in Neuroanatomy, 8, 2014. 1
[26] G.Peyré. Toolbox fast marching. https://www.mathworks.com/matlabcentral/fileexchange/6110-toolbox-fast-marching, 2008. [Online; accessed 19-July-2008]. 10
[27] M. Hassouna and A. Farag. Robust skeletonization using the fast marching method. In Proc. ICIP., 2005. 2
[28] M. Heymann and E. Vanden-Eijnden. The geometric minimum action method: a least action principle on the space of curves. Comm. Pure Appl. Math., 61(8):1052–1117, 2008. 14
[29] Z. Jia, X. Cai, and D. Han. Comparison of several fast algorithms for projection onto an ellipsoid. J. Comput. Appl. Math., 319:320–337, 2017. 14
[30] M. Kass, A. P. Witkin, and D. Terzopoulos. Snakes: Active contour models. Int. J. Comput. Vis., 1:321–331, 2004. 2
[31] R. Kimmel and J. A. Sethian. Optimal algorithm for shape from shading and path planning. J. Math. Imaging Vis., 14(3):237–244, 2001. 1
[32] C. Lenglet, E. Prados, J.-P. Pons, R. Deriche, and O. Faugeras. Brain connectivity mapping using riemannian geometry, control theory, and pdes. SIAM Journal on Imaging Sciences, 2(2):285–322, 2009. 1
[33] P.-L. Lions. Generalized solutions of Hamilton-Jacobi equations. Research Notes in Mathematics, 69. Boston - London - Melbourne: Pitman Advanced Publishing Program, 1982. 1, 3
[34] Y. Liu, Y. Xu, and W. Yin. Acceleration of primal-dual methods by preconditioning and simple subproblem procedures. J. Sci. Comput., 86:21, 2021. 9
[35] S. Luo and J. Qian. Fast sweeping methods for factored anisotropic eikonal equations: multiplicative and additive factors. J. Sci. Comput., 52(2):360–382, 2012. 2
[36] J.-M. Mirebeau. Anisotropic fast-marching on Cartesian grids using lattice basis reduction. SIAM J. Numer. Anal., 52(4):1573–1599, 2014. 2, 10
[37] J.-M. Mirebeau. Efficient fast marching with Finsler metrics. Numer. Math., 126(3):515–557, 2014. 2, 12
[38] J.-M. Mirebeau. Riemannian fast-marching on cartesian grids, using Voronoi's first reduction of quadratic forms. SIAM J. Numer. Anal., 57(6):2608–2655, 2019. 2, 12
[39] D. Mumford and J. Shah. Optimal approximations by piecewise smooth functions and associated variational problems. Commun. Pure Appl. Math., 42(5):577–685, 1989. 2
[40] G. Peyré and L. Cohen. Heuristically driven front propagation for geodesic paths extraction. In Proc. VLSM. 2005. 1, 2, 14
[41] G. Peyré, M. Péchaud, R. Keriven, and L. D. Cohen. Geodesic methods in computer vision and graphics. Found. Trends Comput. Graph. Vis., 5(3-4):197–397, 2009. 1, 2, 14
[42] T. Pock and A. Chambolle. Diagonal preconditioning for first order primal-dual algorithms in convex optimization. In Proc. ICCV, 2011. 8
[43] G. Randers. On an asymmetrical metric in the four-space of general relativity. Phys. Rev., II. Ser., 59:195–199, 1941. 12
[44] R. T. Rockafellar. Convex analysis. Princeton Mathematical Series, No. 28. Princeton University Press, Princeton, N.J., 1970. 6

[45] J. A. Sethian. Level set methods and fast marching methods, volume 3 of Cambridge Monographs on Applied and Computational Mathematics. Cambridge University Press, second edition, 1999. Evolving interfaces in computational geometry, fluid mechanics, computer vision, and materials science. 2
[46] Z. Shen. Lectures on Finsler geometry. Singapore: World Scientific, 2001. 12
[47] A. Telea and J. J. van Wijk. An augmented fast marching method for computing skeletons and centerlines. In Proc. VISSYM, 2002. 2
[48] J. Tsitsiklis. Efficient algorithms for globally optimal trajectories. IEEE Transactions on Automatic Control, 40(9):1528–1538, 1995. 2
[49] H. Xia and P. G. Tucker. Fast equal and biased distance fields for medial axis transform with meshing in mind. Applied Mathematical Modelling, 35:5804–5819, 2011. 1
[50] H. Zhao. A fast sweeping method for eikonal equations. Math. Comput., 74(250):603–627, 2005. 2